

ChemComm

Accepted Manuscript



This article can be cited before page numbers have been issued, to do this please use: Z. Shu, Y. Chen, H. Yu, X. Liao, C. Liu, H. Tang, S. Li and P. Yang, *Chem. Commun.*, 2019, DOI: 10.1039/C9CC01436E.



This is an Accepted Manuscript, which has been through the Royal Society of Chemistry peer review process and has been accepted for publication.

Accepted Manuscripts are published online shortly after acceptance, before technical editing, formatting and proof reading. Using this free service, authors can make their results available to the community, in citable form, before we publish the edited article. We will replace this Accepted Manuscript with the edited and formatted Advance Article as soon as it is available.

You can find more information about Accepted Manuscripts in the [author guidelines](#).

Please note that technical editing may introduce minor changes to the text and/or graphics, which may alter content. The journal's standard [Terms & Conditions](#) and the ethical guidelines, outlined in our [author and reviewer resource centre](#), still apply. In no event shall the Royal Society of Chemistry be held responsible for any errors or omissions in this Accepted Manuscript or any consequences arising from the use of any information it contains.

COMMUNICATION

Supramolecular Catalytic Synthesis of A Novel Bis(salicylaldehyde hydrazone) Ligand for Ratiometric Recognition of AT-DNA

Received 00th January 20xx,
Accepted 00th January 20xxZhengning Shu^{a†}, Yan Chen^{a†}, Hui Yu^b, Xiaoyu Liao^c, Chuanfeng Liu^a, Haodong Tang^a, Sicong Li^a, Peng Yang^{a,c*}

DOI: 10.1039/x0xx00000x

Hydrazone bond formation under physiological condition remains challenging. In this study, a supramolecular catalytic synthesis of bis(salicylaldehyde hydrazone) (2) under physiological condition is described and its AT-DNA ratiometric sensing property is found.

The formation of hydrazone bond is one of the most classical bond-forming reactions. It is widely used in various fields such as organic synthesis, dynamic combinatorial chemistry and pharmacy.¹ This reaction is truly versatile. It could be also applied in bioorthogonal chemistry, which manipulates the biomolecules reactions with small molecules in vitro and in vivo.² However, due to the reversible nature, the relatively low efficiency of this reaction at biological pH should be improved for its realistic application. To solve the problem, the general way is to make use of nucleophilic catalysts such as aniline and their analogous.³ Aside from this traditional method, supramolecular catalysis is recently emerged an alternative strategy.⁴ By using supramolecular macrocycles/cages as the vessels, many reactions take place within their confined hydrophobic cavities.

An ideal supramolecular catalyst should be able to encapsulate the reactant first; stabilize the transition-state next; release the product in the end. In these steps, the host-guest recognition is prerequisite. Toward this end, diverse macrocycles such as cyclodextrins, calixarenes, cucurbiturils, pillarenes as well as various metal-organic assembled cages are developed.⁵ Hosts prefer their own guests and catalyze their unique reactions. In other words, supramolecular macrocycles/cages could serve as specific catalysts. As both amino and aldehydes/ketones are very common species in nature because they are generated through normal and pathogenic metabolism or even oxidative stress,⁶ it is therefore very important to avoid false-positive reactions. In view of this, supramolecular catalysis is a unique strategy for the selective formation of hydrazone bond and deserves more attention.

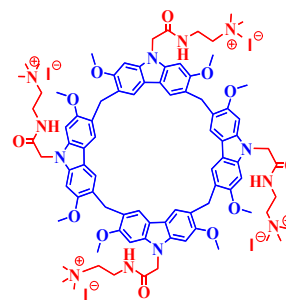
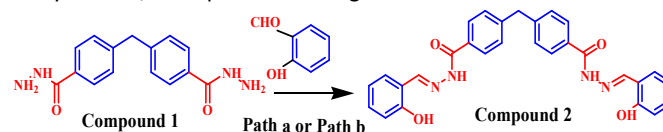


Fig. 1. The water-soluble calix[4]carbazole^{7c} used in this study

In 2016, our group developed a series of carbazole-skeleton macrocycles, namely calix[n]carbazoles.⁷ In the family, 2,7-dimethoxycalix[4]carbazole was synthesized in a decent yield (~25%).^{7b,c} It possesses a large hydrophobic cavity so that it is capable of encapsulating specific guests either in 1,3-alternative^{7c} or in cone conformation^{7d}. In this study, we make further use of the water soluble 2,7-dimethoxycalix[4]carbazole^{7c} (Fig.1) to investigate its capability of serving as a catalyst for the hydrazone-bond forming reaction (Scheme 1). Moreover, in characterization of the bis(salicylaldehyde hydrazone) product (2), we found that it adopted a folded geometry. Based on this unexpected geometry, DNA binding property of 2 was explored and its geometry-switch induced AT-DNA ratiometric sensing property was found in the study. Herein, we report our findings.



Scheme 1. Synthetic routes of 2. Path a): Methanol/Ether, 60 °C; Path b): 10 mM PBS buffer, pH = 7.25, 37 °C

Based on our experiences^{7c,7d}, 1 was used as the reactant to manipulate this catalytic reaction. We firstly carried out the reaction by regular method (Scheme 1, Path a). The reaction worked smoothly and 2 was obtained in the yield of 73.5% (Fig.S1-S4). With 2 at hand and used as a control, we then carried out the reaction via Path b by mixing calix[4]carbazole (0.1 mM, 10% of 1, Mol/Mol) and 1 (1.0 mM) in 10 mM PBS buffer (pH = 7.25, containing 5% DMSO). The reaction was run at 37 °C and was monitored by TLC. The reaction time varied depending on the amount of salicylaldehydes. When salicylaldehyde was less than 9

^aWuyang College of Innovation, Shenyang Pharmaceutical University, Shenyang 110016, China. Email: yangpeng@syphu.edu.cn

^bCollege of Textiles and Clothing, Wuyi University, Jiangmen 529020, China

^cKey Laboratory of Structure-Based Drug Design and Discovery of Ministry of Education, Shenyang Pharmaceutical University, Shenyang 110016 (P. R. China)

Electronic Supplementary Information (ESI) available: The various spectra for the characterization of compounds such as ¹HNMR, ¹³CNMR, HRMS etc. See DOI: 10.1039/x0xx00000x

[†]These authors contributed equally

equivalent of **1**, the reaction was quite slow; higher equivalent salicylaldehyde would speed up the reaction, but it caused inconvenience to purification. The optimized dosage of salicylaldehyde was 9 equivalent. Under this condition, TLC showed that **2** was not produced any further after 8 hours, which meant that the reaction reached the balance due to the reversible nature of hydrazone bond. Stopped the reaction, extracted the solution with CHCl_3 , calix[4]carbazole was easily removed as it was more soluble in water than in CHCl_3 . After purification, **2** was obtained in the yield of 39.7%. This result indicated that the hydrazone bond could be formed by the catalysis of calix[4]carbazole (Path b), although it was not as efficient as the regular method (Path a). As a comparison, the reaction in the absence of calix[4]carbazole barely took place, which illustrated the importance of macrocyclic catalyst.

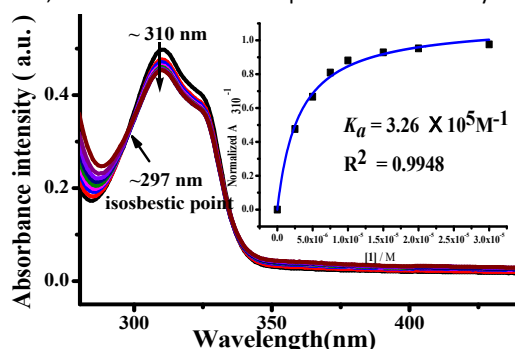


Fig.2 UV-vis spectra of calix[4]carbazole (10 μM) upon addition of **1**; Insertion: Fitted curve of the normalized $A_{310\text{nm}}^{-1}$ as a function of [**1**].

As mentioned earlier, an ideal supramolecular catalyst should bind the reactant to initiate the reaction; it should not bind the product so as to release it. To validate this surmise, we then evaluate the binding properties of calix[4]carbazole to both **1** and **2**. Fig.2 showed that upon binding to **1**, both hypochromic and bathochromic effects of the absorption of calix[4]carbazole at 310 nm occurred with the isosbestic point at 297 nm, an indicative of the specific host-guest binding. The calculated association constant using 1:1 binding model⁸ was $3.26 \times 10^5 \text{ M}^{-1}$, with a satisfactory R^2 value (0.995, see Insertion of Fig.2).

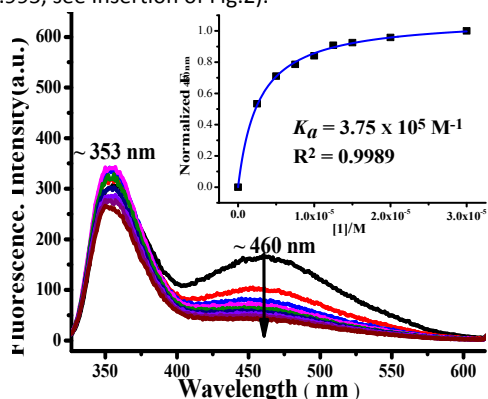


Fig.3 Fluorescence of calix[4]carbazole (10 μM) upon addition of **1**; Insertion: Fitted curve of the normalized $F_{460\text{nm}}$ as a function of [**1**].

Fig.3. showed that the excimer emission (460nm) of the carbazole units of calix[4]carbazole decreased upon addition of **1** whereas its monomer emission at 353nm showed a featureless change. Based on our previous study^{7c}, we proposed that the insertion of **1** into the tubular cavity of calix[4]carbazole quenched the excimer emission by disturbing the face-to-face stacking of 1,3-

alternate calix[4]carbazole. Moreover, **1** also interacted with carbazole unit, which accounted for the featureless monomer emission. In view of this, the current host-guest binding is slightly different from our previously investigated calix[4]carbazole-BPF binding^{7c}. Fitting the curve of the normalized $F_{460\text{nm}}$ as a function of **1**'s concentration using 1:1 model gave the association constant of $3.75 \times 10^5 \text{ M}^{-1}$ with the R^2 value of 0.999 (see Insertion of Fig.3). This result was in agreement with that of UV-vis titration.

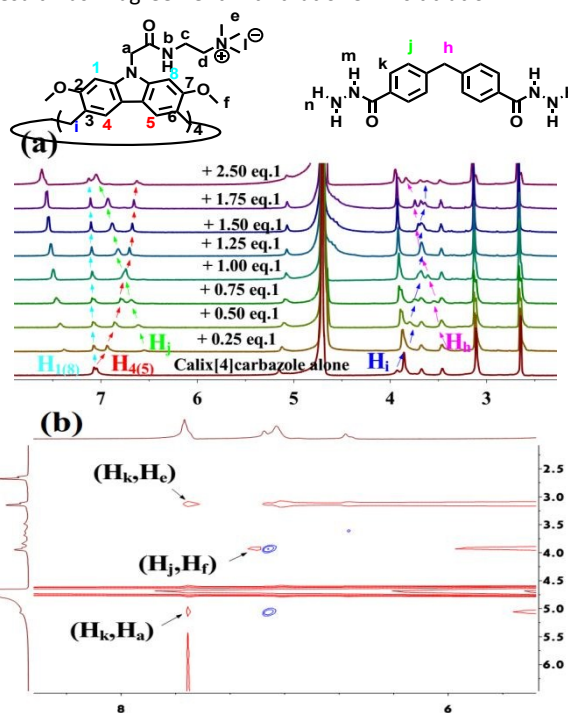


Fig.4 (a) Partial ^1H NMR spectra of calix[4]carbazole upon addition of **1**; (b) Partial 2D NOESY of calix[4]carbazole/**1** complexes.

We further evaluated the binding ability of calix[4]carbazole to **1** by NMR (Fig.4 and Fig.S5). Fig.4a showed that the addition of **1** separated the originally adjoining $\text{H}_{1(8)}$ and $\text{H}_{4(5)}$ from each other: $\text{H}_{1(8)}$ moved toward downfield slightly while $\text{H}_{4(5)}$ remarkably shifted upfield. Moreover, H_i shifted upfield as remarkably as $\text{H}_{4(5)}$ did. The fitted curves of $\text{H}_{4(5)}$ and H_i as a function of $[\text{1}]/[\text{calix4carbazole}]$ ratio also showed 1:1 host-guest binding stoichiometry (Fig.S6 and S7). At 0.25 eq. of calix[4]carbazole, H_j and H_h of **1** were flat (broad) and located at upfield region, an indicative of being shielded nature; at higher equivalents, H_j and H_h remarkably shifted downfield due to the de-shielded feature. Moreover, the correlations of H_k/H_e , H_k/H_a and H_j/H_f were observed in Fig.4b. These results unequivocally indicated the formation of calix[4]carbazole/**1** complexes.

Based on our previous studies⁷, unlike calix[4]carbazole, neither carbazole monomer nor calix[3]carbazole formed a well-define cavity. They would interact with **1** only via "outer-surface π - π stacking" even if they were bound to **1**, which would present a different ^1H NMR spectra from that of the calix[4]carbazole with the inserted **1** in its inner cavity. To verify this surmise, ^1H NMR spectra of both carbazole monomer and calix[3]carbazole upon addition to **1** were recorded, respectively (Fig.S8 and S9), The result showed that the addition of **1** neither changed the chemical shift of protons of carbazole monomer nor changed those of calix[3]carbazole,

which further illustrated that **1** was encapsulated by the well defined cavity of calix[4]carbazole.

Having found that calix[4]carbazole encapsulated **1**, we then examined its binding property to **2** (the product). Fig.S10 showed that the addition of **2** caused remarkable light scattering UV-vis spectra of calix[4]carbazole. It indicated the formation of large particles in the current solution, which was verified by DLS titration (Fig.S11). Based on other groups' experiences⁵ and ours^{7c,d}, the solubility of a guest could be enhanced by a water soluble host if they bound to each other, vice versa. As such, the above result indicated that calix[4]carbazole did not bind to the product. It thus revealed the reason for calix[4]carbazole-catalyzed synthesis of **2**.

In the characterization of **2**, its irregular fluorescent spectrum drawn our attention and promoted us to further investigate its property. In brief, its λ_{\max} was 336 nm (Fig.S12), the emission peak appeared at 520 nm (Fig.S13), its Stokes shift was 184 nm. It surprised us not because of its large Stokes shift but because of the emission at 520 nm. It is generally accepted that the compounds composed of hydrazone bonds were non-emissive and became emission only when the bonds' free rotation was restricted.⁹ Our own control experiment also showed that the mono-salicylaldehyde hydrazone (Fig.S14) was non-fluorescent under the current condition (Fig.S15). As such, we then proposed that the fluorescence at 520 nm resulted from either the intramolecular stacking chromophores or the intermolecular stacking ones. The latter possibility was soon precluded because the absorbance of **2** was dependent linearly with its concentration (Fig.S16).

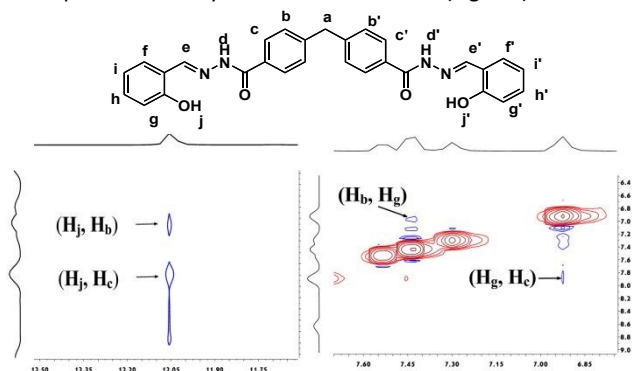


Fig.5 Partial 2D NOESY spectrum of **2**.

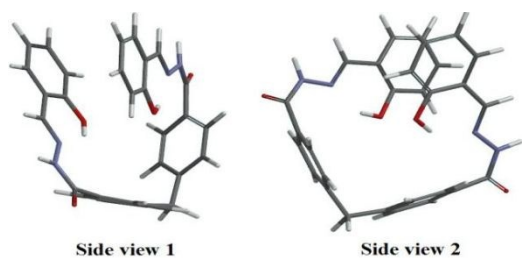


Fig.6 Energy-minimized model of **2** (C=dark gray,H=light gray,N=blue,O=red)

2D NOESY of **2** (Fig.5 and Fig.S17) further illustrated its intramolecular stacking pattern due to the observed correlations of H_j/H_b , H_j/H_c , H_g/H_b and H_g/H_c . In view of the relative far distances between these proton pairs, these correlations took place most possibly between the two symmetrical sides due to the folded structure of **2**. An energy-minimized molecular model of **2** (Fig.6) revealed its unique geometry: two salicylaldehyde hydrazone units were folded along C_2 -axis of diphenylmethane unit, which produced the face-to-face stacked chromophores. This model agreed well

with the results from both NMR and fluorescent studies. Engineering the switch of folded/unfolded geometries of a molecule is one of popular principles for the design of ratiometric sensors. This inspired us to investigate the potential of **2** serving as a sensor. Based on our experiences^{7e,7f,10}, the methylene-bridged compounds often exhibited AT-DNA binding ability. With this idea in minds, the AT-DNA binding properties of **2** were determined. Fig.7 showed that the absorbance of **2** at 336 nm was hypochromic and bathochromic accompanying with the isosbestic point at 299 nm. This pattern usually meant the binding event occurred at the DNA grooves. The calculated association constant using 1:1 binding model was $2.97 \times 10^4 M^{-1}$ with R^2 value of 0.993 (see Insertion of Fig.7). This binding strength was relatively weak compared to those of the most reported DNA-ligands interactions, which might account for its less significant changes of cotton effects at both 275 nm and 250 nm in its CD titration spectra (Fig.S18). As we know, most of DNA ligands usually possess binding strength higher than $10^5 M^{-1}$ because they often contain positively charged amino group, which interact electrostatically with DNA phosphate anions. However, **2** does not contain any positively charged functional group and it is a uncharged "neutral" molecule, which may account for its relatively weak DNA binding strength.

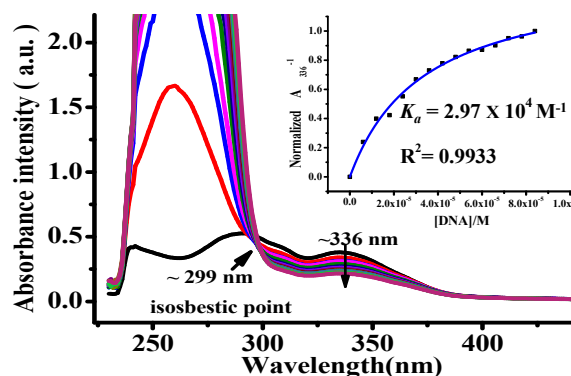


Fig.7 UV-vis spectra of **2** (20 μM) upon addition of 12AT; Insertion: Fitted curve using the normalized $A_{336 nm}^{-1}$ as a function of DNA concentration

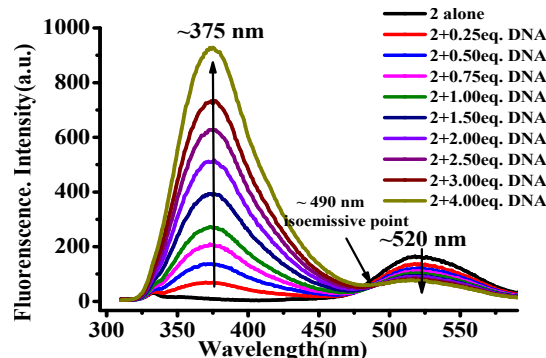


Fig.8. Fluorescence spectra of **2** (5 μM) upon addition of 12AT

The fluorescent spectra of **2** upon addition of DNA (Fig.8) showed that the emission at 520nm quenched gradually whereas the intensity at 375 nm was remarkably enhanced; the isoemissive point appeared at 490 nm. The fitted curve of fluorescence as a function of **2**' concentration also showed 1:1 binding of **2** to 12AT (Fig.S19). This result indicated that the original folded geometry of **2** was unfolded upon binding to AT-DNA so that its excimer's emission decreased while its monomer's emission increased, a typical spectral pattern of a ratiometric sensor.

In order to gain insight of AT-selective binding nature, three other different sequenced duplex DNA were examined. Fig.9 showed that both drew DNA¹¹ and 8AT quenched the fluorescence at 520 nm and enhanced the emission at 375 nm, to different extents; however, the addition of 12GC only quenched the fluorescence at 520 nm but barely changed the emission at 375nm. The curve of F_{375}/F_{520nm} as a function of $[DNA]/[2]$ ratio was then plotted (Fig.9d). Basically, within one periodical length of A-tracts DNA (10-12 base pairs)¹², the more AT base pair DNA contained, the more significant the slope of titration curve was, which indicated that **2** was an AT-DNA selective ligand.

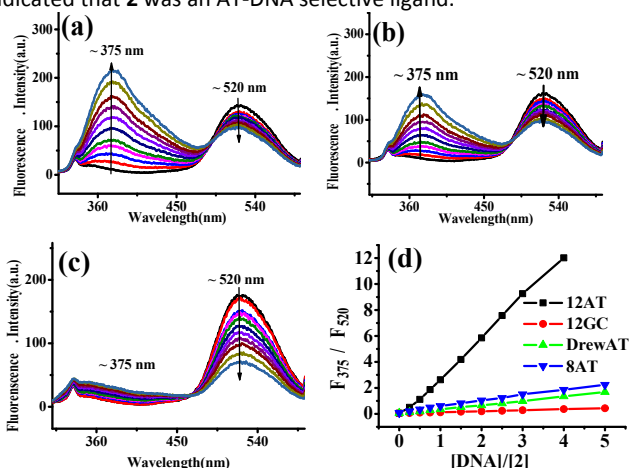


Fig.9. Fluorescence of **2** (5 μ M) upon addition of (a) 8AT; (b) drewAT; (c) 12GC; $[DNA]/[2]$ ratio: 0.25, 0.50, 0.75, 1.0, 1.50, 2.0, 2.5, 3.0, 4.0 (d) plotted curve using F_{375}/F_{520nm} as a function of the ratio of $[DNA]/[2]$.

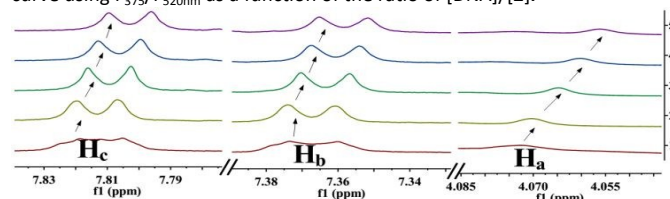


Fig.10 Partial ¹H NMR spectra of **2** upon addition of 12AT (Line 1: **2** alone; Line 2: **2**+0.25eq.DNA; Line 3: **2**+0.5eq.DNA; Line 4: **2**+0.75eq.DNA; Line 5: **2**+1.0eq.DNA)

In the end, ¹H NMR spectra of **2** upon addition of AT-DNA were recorded to give a view of potential binding mode. The partial spectra were listed in Fig.10 (please see full spectra in Fig. S20). Due to the H/D exchange, unfortunately, we did not observe the protons of both OH and NH of **2**. What had been seen was that the addition of DNA made H_a , H_b and H_c of **2** move slightly towards upfield while the other protons of **2** barely changed. This result indicated that **2**-DNA binding probably took place in a way that the edge of diphenylmethane unit was inserted into the minor groove of AT-DNA due to the hydrophobic binding whereas the two salicylaldehyde hydrazone units interacted with the un-paired carbonyl group of thymine of AT-DNA due to hydrogen bonding.

In conclusion, a bishydrazone compound was synthesized under physiological condition using calix[4]carbazole as a supramolecular catalyst. This molecule adopted a folded geometry and exhibited an intramolecular excimer emission. By engineering the switch from the folded to the unfolded geometry, this molecule could serve as an AT-DNA selective ratiometric sensor.

The current work is not very satisfying and further work still remains: the efficiency of supramolecular catalytic reaction needs

to be improved; the water solubility of **2** should be enhanced in order to make it more applicable. Nevertheless, our work is one of the few cases that supramolecular catalyzed hydrazone-formation reaction. Moreover, **2** represents a novel geometry-switch induced uncharged AT-DNA probe. In view of these two points, our findings may shed light on the assessment of catalytic properties of more supramolecular macrocycles and pave the way for the search of geometry-switchable "neutral" DNA ratiometric sensors.

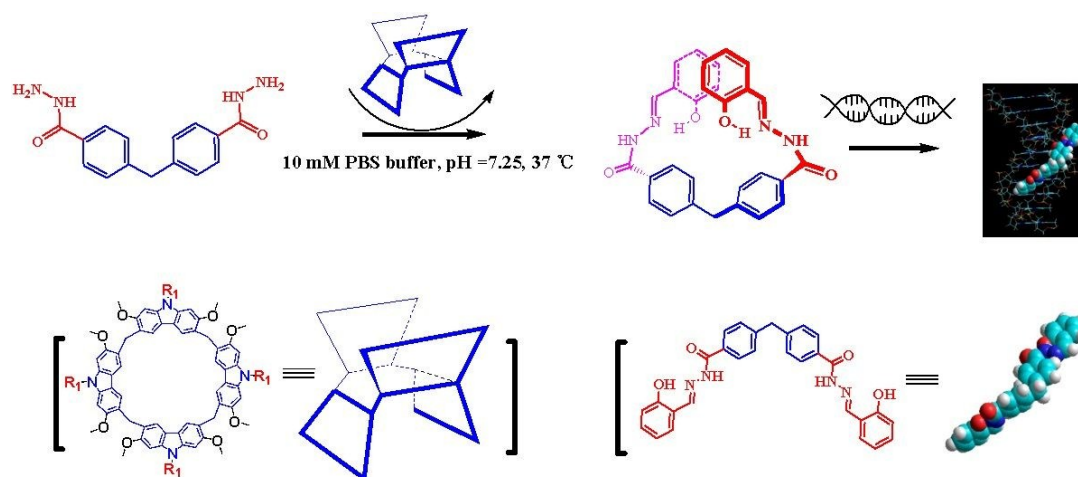
We thank Natural Science Foundation of Liaoning Province (20180550874), Foundation of Higher Education of Guangdong (2016KTSCX146), Natural Science Foundation of Guangdong Province (2018A0303130245).

Conflicts of interest

There are no conflicts to declare.

Notes and references

- (a) S. Kobayashi, Y. Mori, J. S. Fossey, M. M. Salter, *Chem. Rev.*, 2011, **111**, 2626; (b) P. T. Corbett, J. Leclair, L. Vial, K. R. West, J. L. Wietor, J. K. Sanders, S. Otto, *Chem. Rev.*, 2006, **106**(9), 3652; (c) R. Corbett Narang, B. Narasimhan, S. Sharma, *Curr. Med. Chem.*, 2012, **19**, 569.
- E. M. Sletten, C. R. Bertozzi, *Angew. Chem., Int. Ed.* 2009, **48**, 6974.
- D. K. Kölmel, E. T. Kool, *Chem. Rev.*, 2017, **117**(15), 10358
- (a) C. J. Brown, F. D. Toste, R. G. Bergman, K. N. Raymond, *Chem. Rev.* 2015, **115**(9), 3012; (b) Y. Yu, Jr. J. Rebek, *Acc. Chem. Res.*, 2018, **51** (12), 3031.
- (a) R. Breslow, S. D. Dong, *Chem. Rev.*, 1998, **98**, 1997; (b) D. M. Homden, C. Redshaw, *Chem. Rev.*, 2008, **108**, 5086; (c) J. Lagona, P. Mukhopadhyay, S. Chakrabarti, L. Isaacs, *Angew. Chem., Int. Ed.* 2005, **44**, 4844; (d) T. Ogoshi, T. Yamagishi, Y. Nakamoto, *Chem. Rev.*, 2016, **116**(14), 7937; (e) T. R. Cook, Y. R. Zheng, P. J. Stang, *Chem. Rev.*, 2013, **113** (1), 734.
- (a) L. Laffel, *Diabetes/Metab. Res. Rev.* 1999, **15**, 412; (b) S. Dalleau, M. Baradat, F. Gueraud, L. Huc, *Cell Death Differ.* 2013, **20**, 1615.
- (a) P. Yang, Y. Jian, X. Zhou, G. Li, T. Deng, H. Y. Shen, Z. Z. Yang, Z. M. Tian, *J. Org. Chem.*, 2016, **81**(7), 2974; (b) X. Zhou, G. Li, P. Yang, L. Zhao, T. Deng, H. Y. Shen, Z. Z. Yang, Z. M. Tian, Y. Chen, *Sensor. Actuat. B-Chemical*, 2017, **242**, 56; (c) G. Li, L. Zhao, P. Yang, Z. Z. Yang, Z. M. Tian, Y. Chen, H. Y. Shen, C. Hu, *Anal. Chem.*, 2016, **88**(21), 10751; (d) L. Zhao, L. Kang, Y. Chen, G. Li, L. Wang, C. Hu, P. Yang, *Spectrochim. Acta A Mol Biomol Spectrosc.* 2018, **193**, 276; (e) G. Li, X. Song, H. Yu, C. Hu, M. Liu, J. Cai, L. Zhao, Y. Chen, P. Yang, *Sensor. Actuat. B* 2018, **259**, 177; (f) Z. Z. Yang, Y. Chen, G. Li, Z. M. Tian, L. Zhao, X. Wu, Q. Ma, M.-Z. Liu, P. Yang, *Chem.-Eur. J.*, 2018, **24** (23), 6087
- A. Connors, *Binding Constants*, Wiley, New York, 1987.
- (a) S. Anbu, R. Ravishankaran, M. F. Guedes da Silva, A. A. Karande, A. J. Pombeiro, *Inorg. Chem.*, 2014, **53** (13), 6655; (b) K. Li, Y. Xiang, X. Wang, J. Li, R. Hu, A. Tong, B. Z. Tang, *J. Am. Chem. Soc.*, 2014, **136** (4), 1643
- G. Li, X. Zhou, P. Yang, Y. Jian, T. Deng, H. Shen, Y. Bao, *Tetrahedron Lett.* 2014, **55**, 7054.
- B. Dumat, G. Bordeau, E. Faurel-Paul, F. Mahuteau-Betzer, N. Saettel, G. F. Metge, C. Fiorini-Debuisschert, F. Charra, M. P. Teulade-Fichou, *J. Am. Chem. Soc.*, 2013, **135** (34), 12697.
- (a) M. Y. Tolstorukov, K. M. Virnik, S. Adhya, V. B. Zhurkin, *Nucleic Acids Res.* 2005, **33**, 3907; (b) E. N. Trifonov, J. L. Sussman, *Proc. Natl. Acad. Sci. U. S. A.* 1980, **77**, 3816.



A bis-hydrazone compound (**2**) is synthesized via supramolecular catalysis under physiological condition and its AT-DNA ratiometric sensing property is found.